catalysts

MDPI

Supplementary Materials

Constructing Stable MoO_x-NiS_x Film via Electrodeposition and Hydrothermal Method for Water Splitting

Shihu Zhu [1,2], Tiantian Liu [1,3], Shuang Yu [1,3], Huijing Yang [1,3], Qimeng Sun [1,3] and Jin You Zheng [1,3,*]

[1] Engineering Research Center of Advanced Functional Material Manufacturing of Ministry of Education, School of Chemical Engineering, Zhengzhou University, Zhengzhou 450001, China; 15638216421@163.com (S.Z.); ltt13429817116@163.com (T.L.); shuangyu_225@163.com (S.Y.); huiging@163.com (H.Y.); qimeng_sun1@163.com (Q.S.)
[2] School of Mechanical and Power Engineering, Zhengzhou University, Zhengzhou 450001, China
[3] National Key Laboratory of Coking Coal Green Process Research, Zhengzhou University, Zhengzhou 450001, China
* Correspondence: jinyouzh@zzu.edu.cn

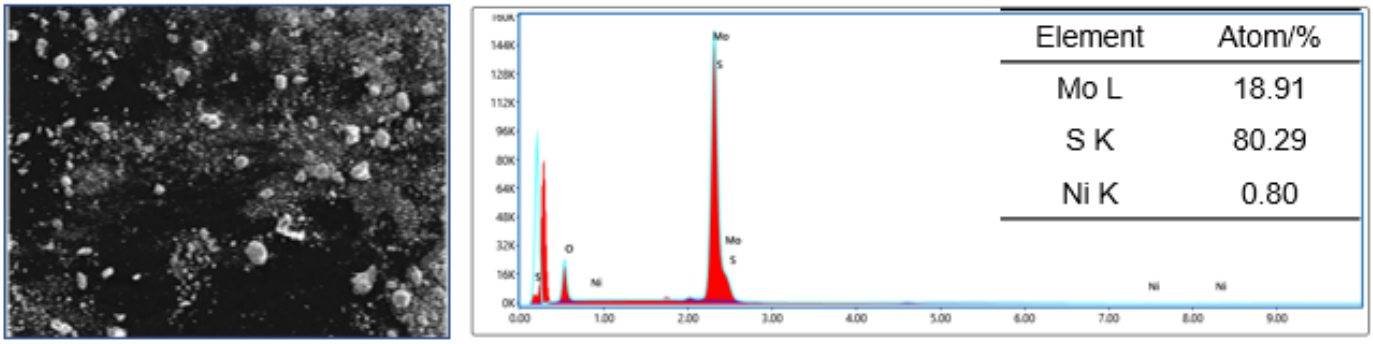

Figure S1. EDS spectrum of the 1H5E-CC intermediate products.

1H5E-CC was prepared by electrodeposition and hydrothermal reaction, finally we collected the precipitate. The deposition bath containing 0.05 M Na_2SO_4, 0.5 M H_3BO_3, and 0.1 M Na_2SO_4, and depositing was performed at room temperature in constant current way at −100 mA for 5 min. Then 0.01 M ammonium tetrathiomolybdate and 0.5 M thiourea were dissolved in 50 mL DI water, and the mixed solution was stirred at room temperature for 30 min. Then sample and mixed solution were transferred into a 100 mL Teflon-lined stainless steel autoclave and maintained at 180 °C for 1 h. In the end, collecting the precipitate by suction filtration and drying.

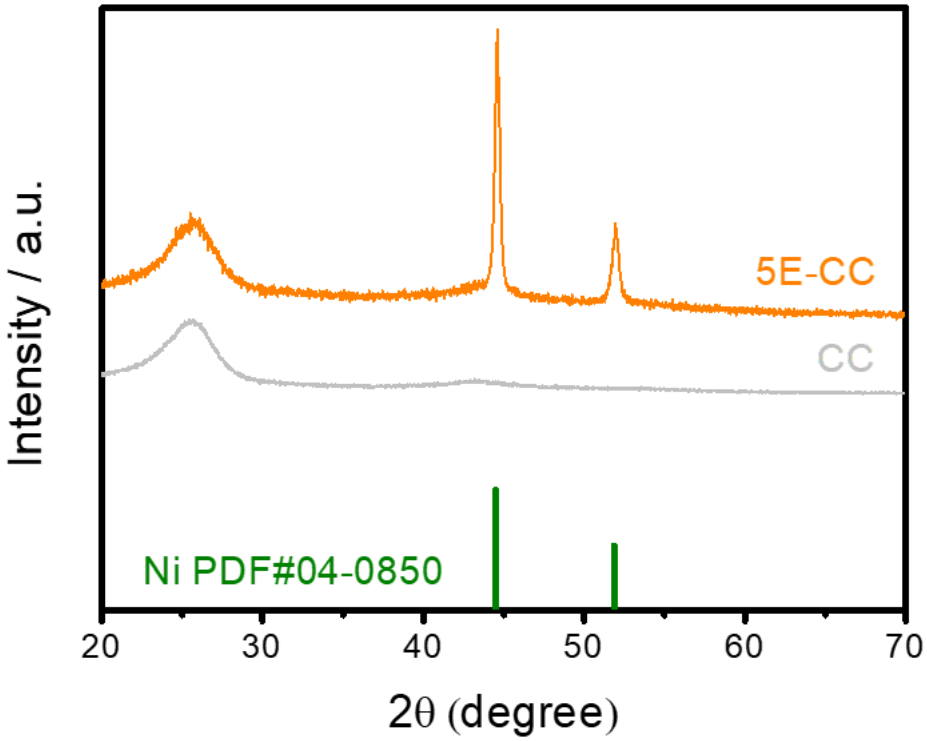

Figure S2. XRD patterns of 5E-CC and CC.

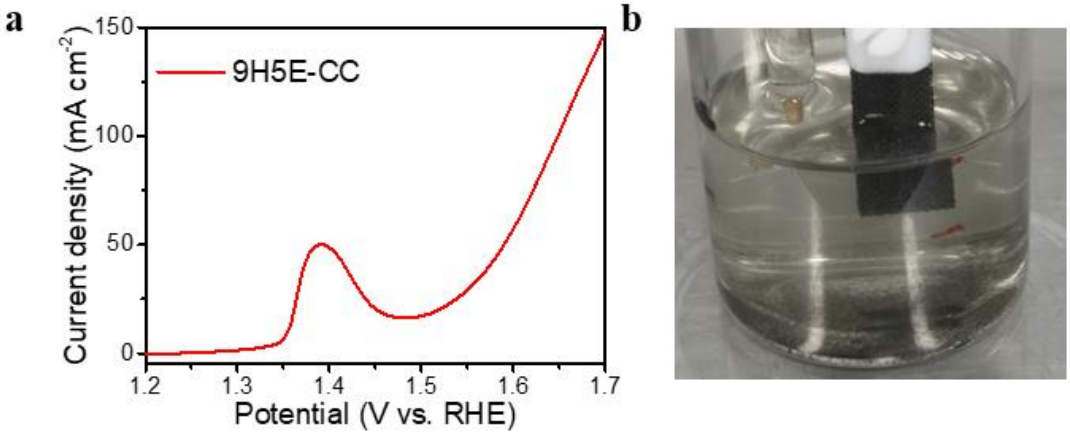

Figure S3. Polarization curve of 9H5E-CC for OER. (a) Polarization curve, (b) Photographic image of 9H10E-CC at OER process.

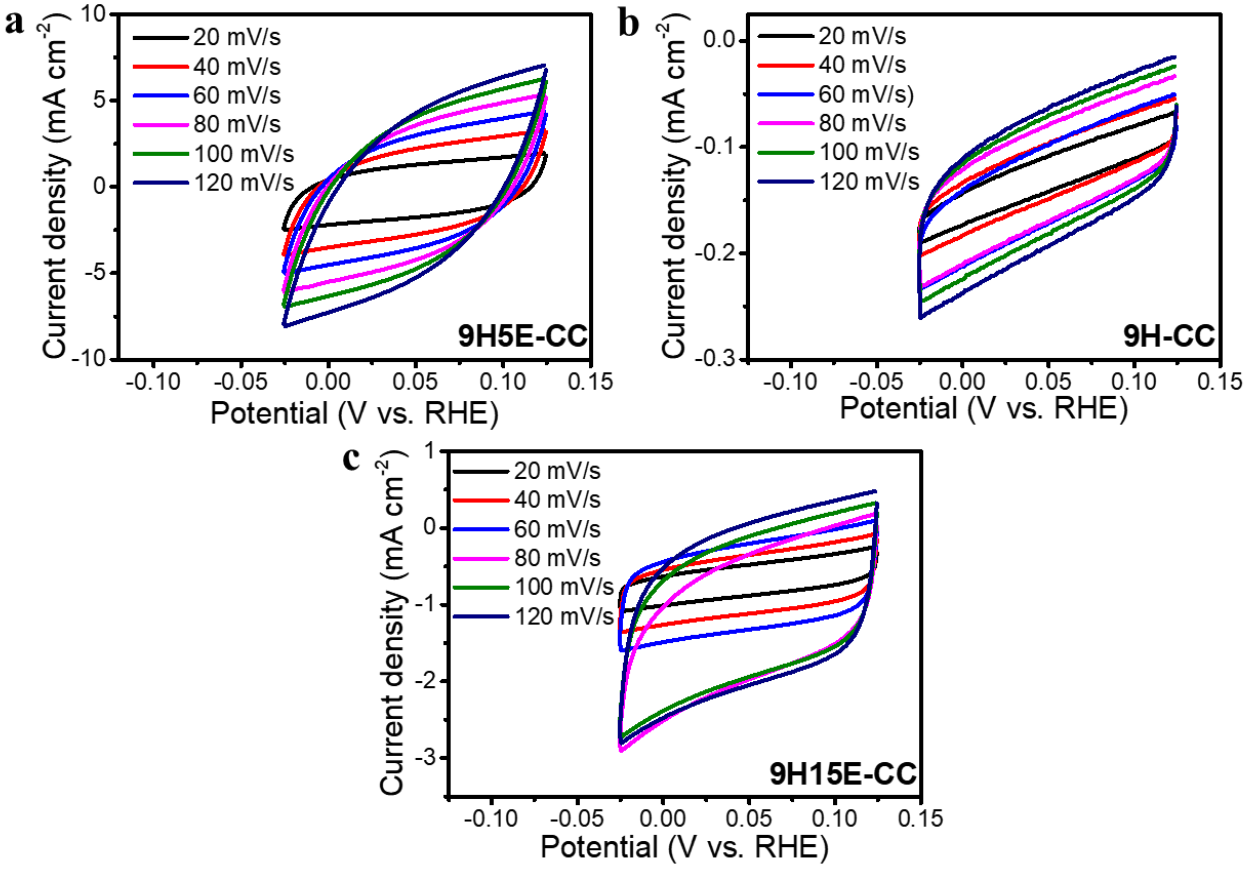

Figure S4. CV curves showing the capacitive of C_{dl} of (a) 9H5E-CC, (b) 9H-CC, and (c) 9H15E-CC.

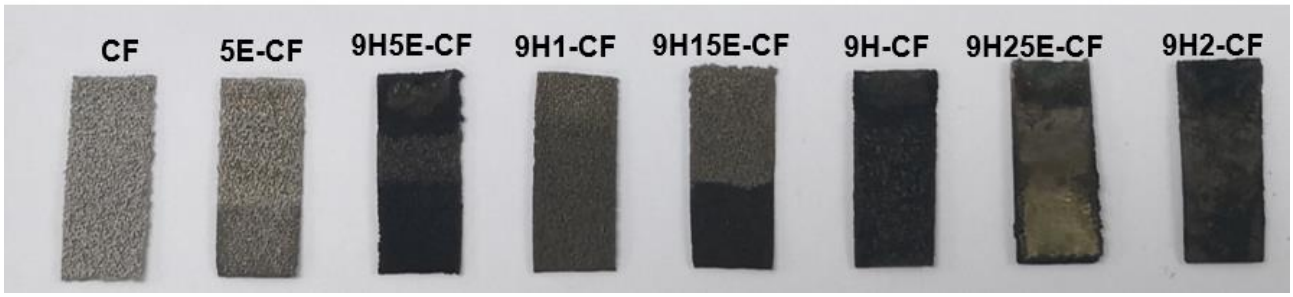

Figure S5. Photographic images of the as-prepared samples on CF.

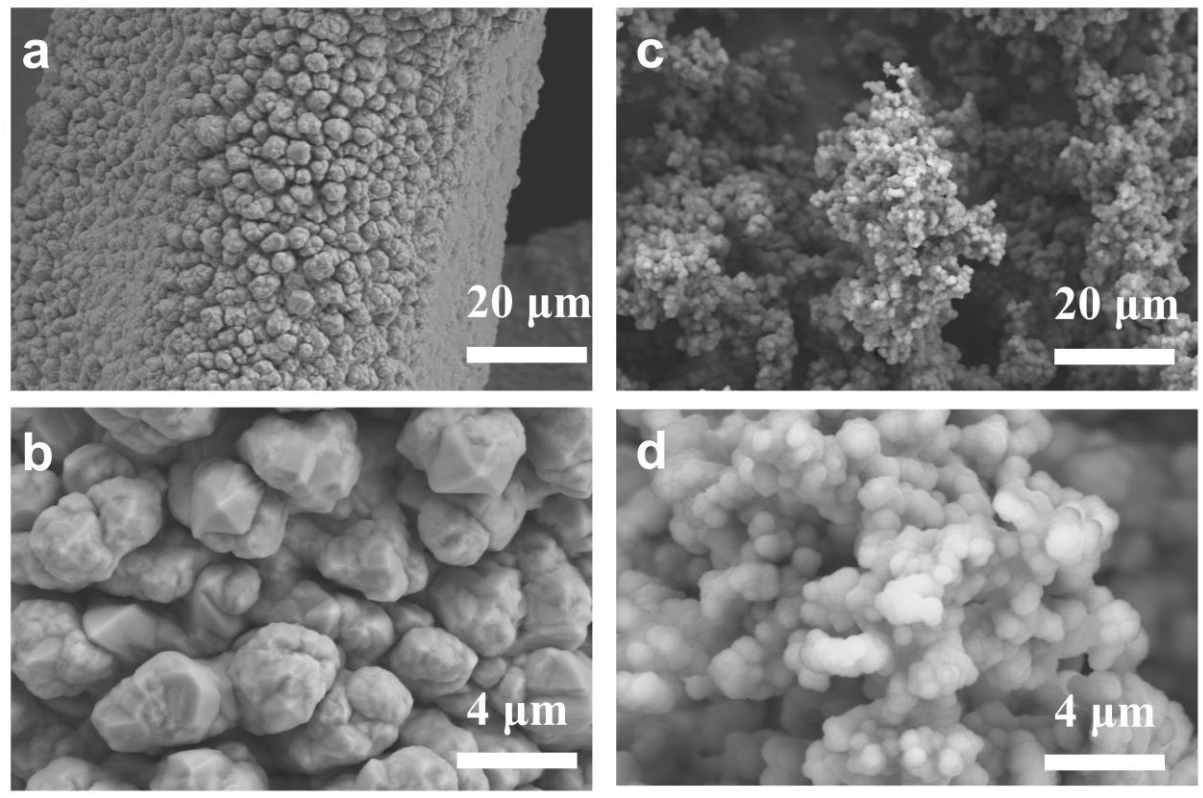

Figure S6. SEM images of (a, e) 5E-CF and (c, d) 9H5E-CF before polarization.

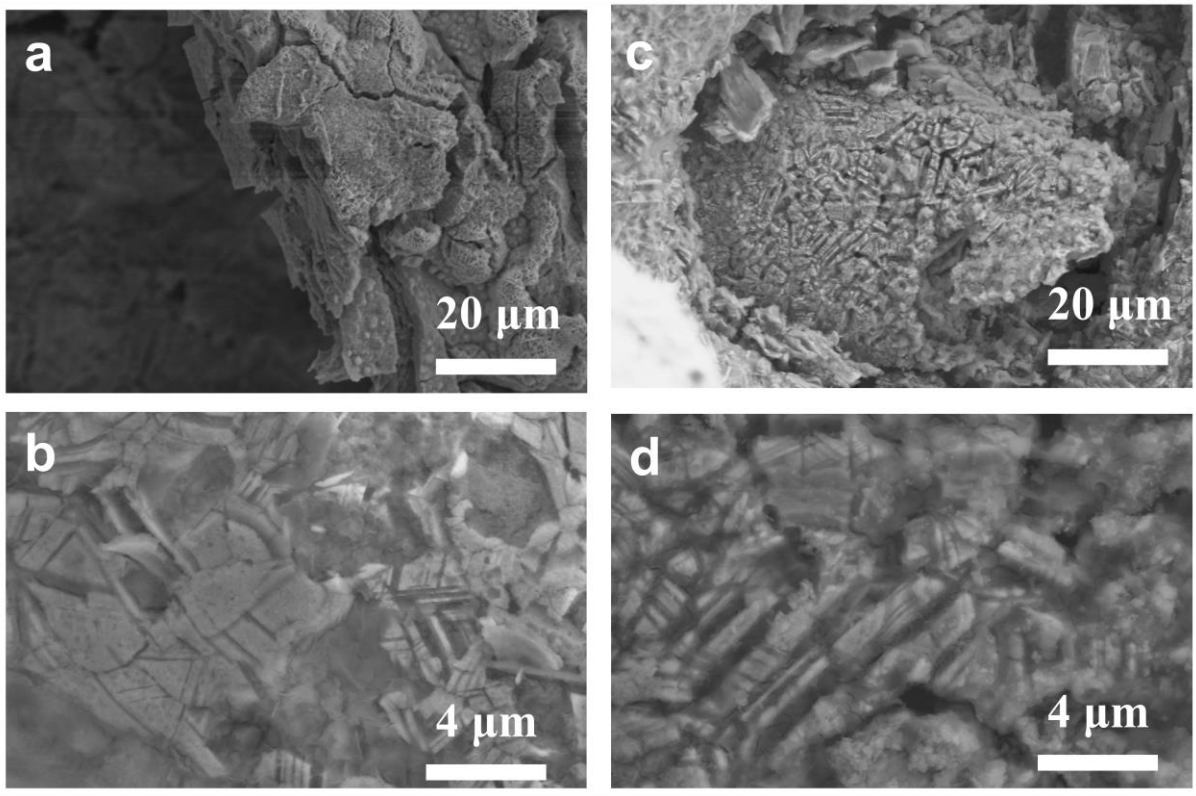

Figure S7. SEM images of 9H5E-CF (c, g) before and (c, d) after running chronopotentiometry.

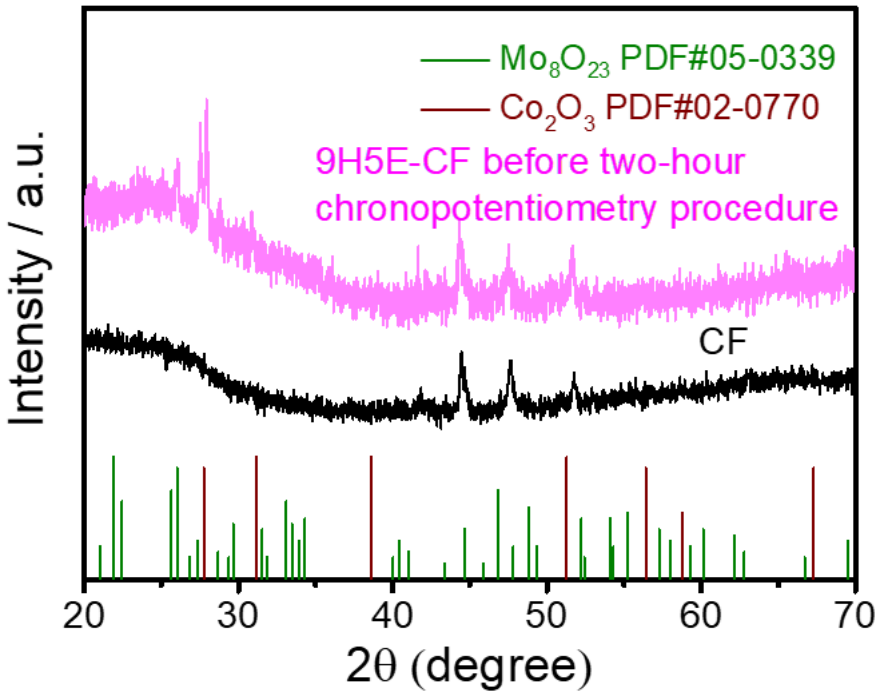

Figure S8. XRD of 9H5E-CF before 2 h-chronopotentiometry procedure.

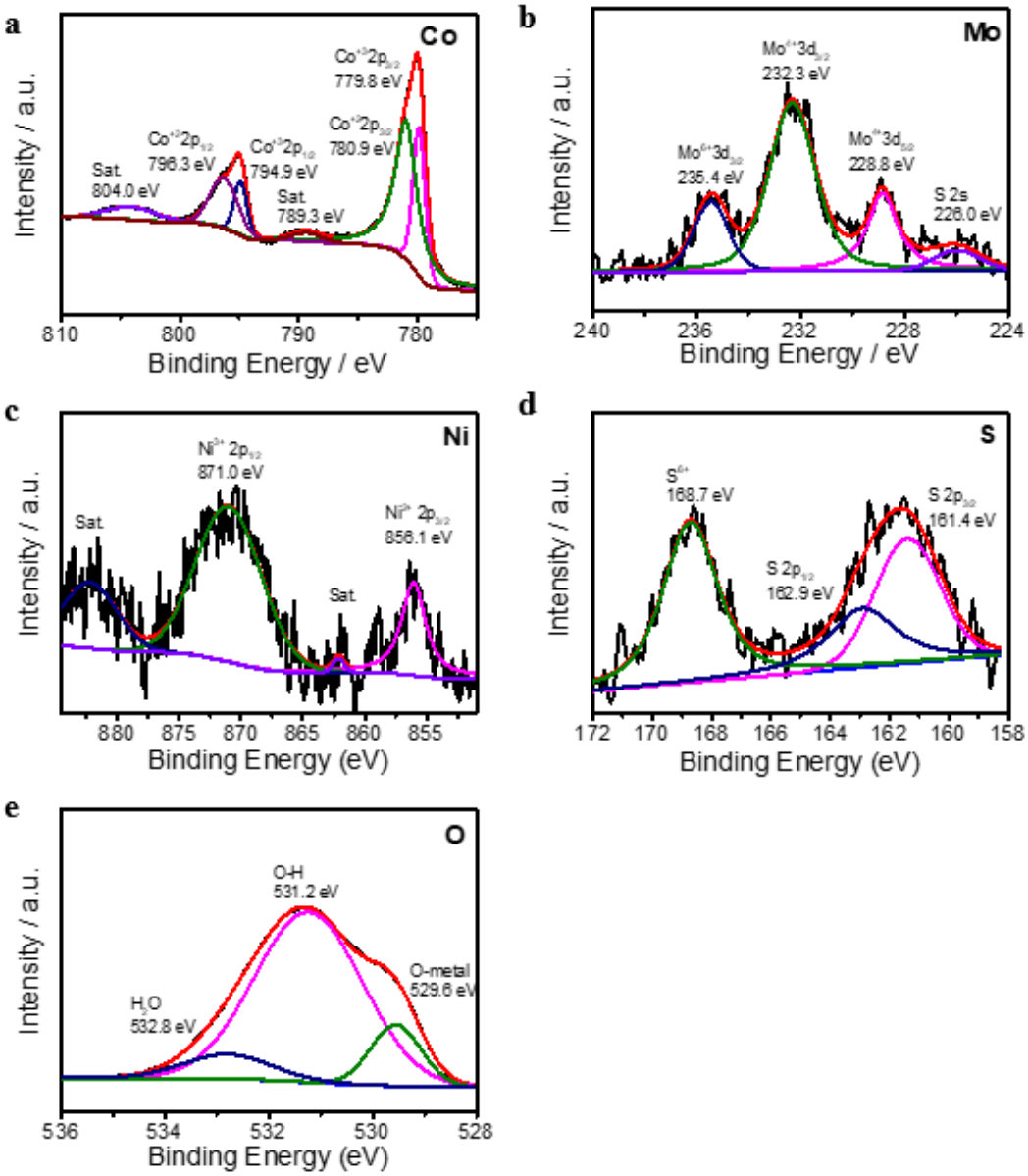

Figure S9. XPS spectra of (a) Co element (b) Mo element (c) Ni element (d) O element (e) S element for 9H5E-CF.

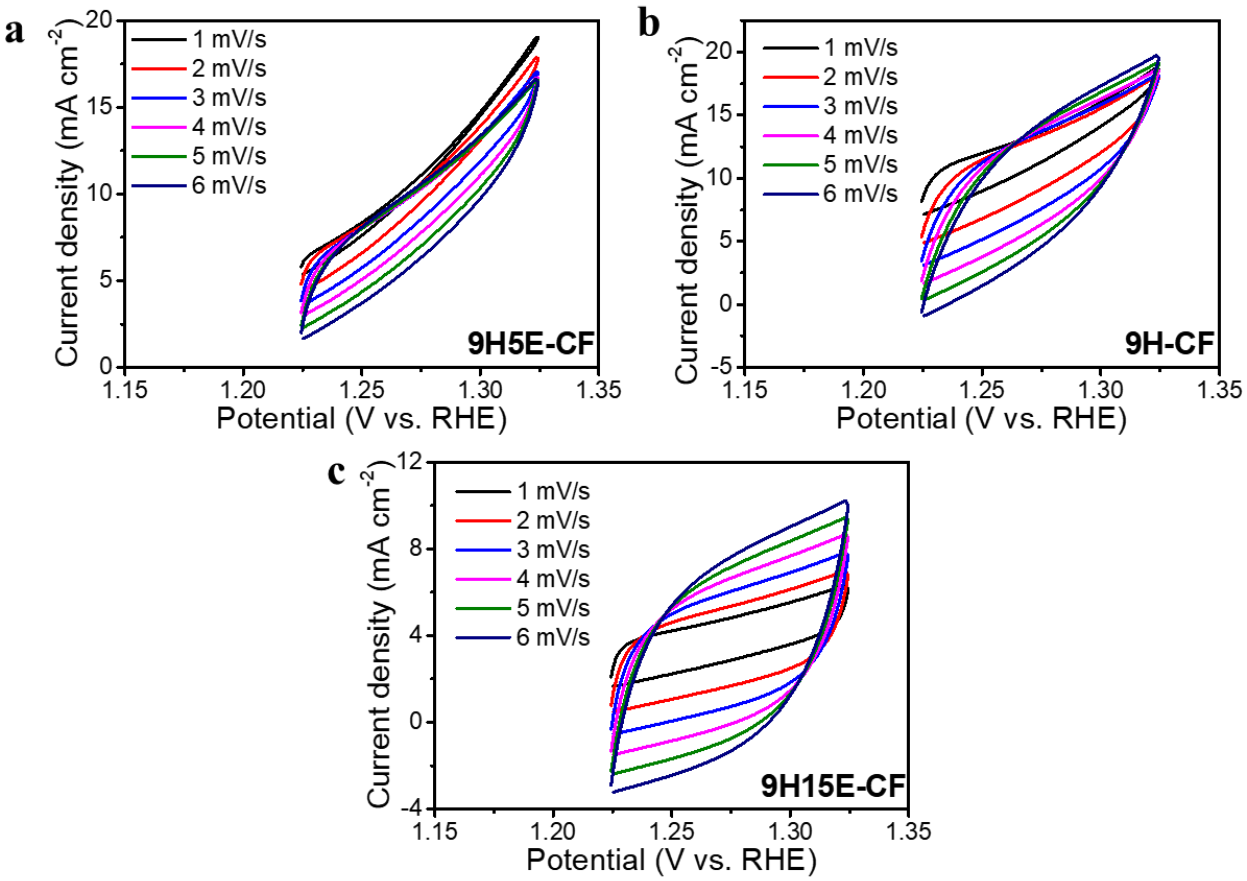

Figure S10. CV curves showing the capacitive of C_{dl} of (a) 9H5E-CF, (b) 9H-CF, and (c) 9H15E-CF.

Table S1. Listing of the experimental parameters for fabricating the samples.

Samples	Substrate	Experimental parameters	
		Electrodeposition time (at −100 mA)	Hydrothermal reaction solution (180 °C for 9 h)
CC	CC		
5E-CC	CC	5 min	
9H5E-CC	CC	5 min	0.5 M CH_4N_2S, 0.01 M $(NH_4)_2MoS_4$, 50 mL H_2O
9H1-CC	CC		0.5 M CH_4N_2S, 50 mL H_2O
9H15E-CC	CC	5 min	0.5 M CH_4N_2S, 50 mL H_2O
9H-CC	CC		0.5 M CH_4N_2S, 0.01 M $(NH_4)_2MoS_4$, 50 mL H_2O
9H25E-CC	CC	5 min	0.01 M $(NH_4)_2MoS_4$, 50 mL H_2O
9H2-CC	CC		0.01 M $(NH_4)_2MoS_4$, 50 mL H_2O
CF	CF		
5E-CF	CF	5 min	
9H5E-CF	CF	5 min	0.5 M CH_4N_2S, 0.01 M $(NH_4)_2MoS_4$, 50 mL H_2O
9H1-CF	CF		0.5 M CH_4N_2S, 50 mL H_2O
9H15E-CF	CF	5 min	0.5 M CH_4N_2S, 50 mL H_2O
9H-CF	CF		0.5 M CH_4N_2S, 0.01 M $(NH_4)_2MoS_4$, 50 mL H_2O
9H25E-CF	CF	5 min	0.01 M $(NH_4)_2MoS_4$, 50 mL H_2O
9H2-CF	CF		0.01 M $(NH_4)_2MoS_4$, 50 mL H_2O

Table S2. R_s and R_{ct} value of 9H5E-CC, 9H-CC and 9H15-CC.

Electrode	R_s	R_{ct} (Ω)
9H5E-CC	2.145	1.325
9H-CC	2.061	1.799
9H15E-CC	2.146	1.377

Table S3. R_s and R_{ct} value of 9H5E-CF, 9H-CF and 9H15-CF.

Electrode	R_s	R_{ct} (Ω)
9H5E-CF	1.614	1.527
9H-CF	1.909	2.301
9H15-CF	1.757	1.653

Table S4. Comparison of the water splitting performance of the catalyst in this work with other reported bifunctional catalysts in 1 M KOH (References [39-51] are cited in the supplementary materials).

Catalysts	Overpotential of HER	Overpotential of OER	Voltage of overall water splitting at current density j	Ref.
MoO_3-NiS_x	η_{10} = 142 mV	η_{50} = 294 mV	η_{50} = 1.88 V	This work
MoS_2@Ni_9S_8/Co_3S_4	η_{10} = 81.24 mV	η_{50} = 159.67 mV	η_{10} = 1.45 V	1
CoS_2/MoS_2	η_{10} = 53 mV	η_{10} = 255 mV	η_{10} = 1.55 V	2
Li-α-MoO_3/CFP		η_{10} = 458 mV		3
$Co_3(PO_4)_2$-MoO_3-x/$CoMoO_4$/NF	η_{100} = 76 mV			4
Fe-NiCoP-MoO_3	η_{10} = 65 mV	η_{50} = 293 mV	η_{10} = 1.586 V	5
p-MoS_2/NiS_2	η_{10} = 155 mV	η_{100} = 337 mV	η_{10} = 1.51 V	6
NiS/FeS_2	η_{10} = 148 mV	η_{10} = 183 mV	η_{10} = 1.56 V	7
ZneNiS-3	η_{10} = 208 mV	η_{50} = 302 mV	η_{50} = 1.71 V	8
CoS/NiS@CuS	η_{10} = 110 mV			9
NiO/Co_2P NSs	η_{10} = 108 mV	η_{10} = 207 mV	η_{10} = 1.57 V	10
FeS/NiS and Ni/NiO	η_{10} = 84 mV	η_{10} = 168 mV	η_{10} = 1.47 V	11
NiS/$NiCo_2S_4$	η_{10} = 198 mV	η_{10} = 259 mV		12
NiS/N–C	η_{10} = 88 mV	η_{10} = 170 mV	η_{10} = 1.51 V	13

References

1. Pei, Z.; Qin, T.; Tian, R.; Ou, Y.; Guo, X. Construction of an Amethyst-like MoS_2@Ni_9S_8/Co_3S_4 Rod Electrocatalyst for Overall Water Splitting. *Nanomaterials* **2023**, *13*, 2302.
2. Qian, Y.; Yu, J.; Zhang, F.; Fei, Z.; Shi, H.; Kang, D.J.; Pang, H. Hierarchical Binary Metal Sulfides Nanoflakes Decorated on Graphene with Precious-Metal-like Activity for Water Electrolysis. *Chem. Eng. J.* **2023**, *470*, 144372.
3. Feng, L.; Zhou, J.; Xiao, J.; Chen, F.; Zhao, Z.; Liu, M.; Zhang, N.; Gao, F. Simple Cathodic Deposition of FeS/NiS-Activated Ni/NiO Heterojunctions for High-Concentration Overall Water Splitting Reactions. *Int. J. Hydrogen Energy* **2023**, *48*, 29852–29864.
4. Wan, Z.; Zhang, Y.; Ren, Q.; Li, X.; Yu, H.; Zhou, W.; Ma, X.; Xuan, C. Interface Engineering of NiS/$NiCo_2S_4$ Heterostructure with Charge Redistribution for Boosting Overall Water Splitting. *J. Colloid Interface Sci.* **2024**, *653*, 795–806.
5. Liu, Z.; Jia, H.; Wang, H.; Wang, Y.; Zhang, G. Constructing S-Deficient Nickel Sulfide/N-Doped Carbon Interface for Improved Water Splitting Activity. *Nanoscale* **2023**, 16039–16048.
6. Kim, K.H.; Hong, D.; Kim, M.G.; Choi, W.; Min, T.; Kim, Y.M.; Choi, Y.H. Improving Electrocatalytic Activity of MoO_3 for the Oxygen Evolution Reaction by Incorporation of Li Ions. *ACS Mater. Lett.* **2023**, *5*, 1196–1201.
7. Yang, M.; Shi, B.; Tang, Y.; Lu, H.; Wang, G.; Zhang, S.; Sarwar, M.T.; Tang, A.; Fu, L.; Wu, M.; et al. Interfacial Chemical Bond Modulation of $Co_3(PO_4)_2$-MoO_{3-x} Heterostructures for Alkaline Water/Seawater Splitting. *Inorg. Chem.* **2023**, *62*, 2838–2847.
8. Guo, F.; Li, W.; Liu, Y.; Chen, Q.; Zhong, Q. Heterogeneous Fe-Doped NiCoP-MoO_3 Efficient Electrocatalysts for Overall Water Splitting. *Langmuir* **2023**, 39, 1042–1050.
9. Yu, N.; Ke, H.; Yu, H.; Wu, X.; Li, S.; Chen, G.; Wang, J.; Cai, N.; Xue, Y.; Yu, F. Polysulfide-Induced Synthesis of Coral-Like MoS_2/NiS_2 Nanostructures for Overall Water Splitting. *ACS Appl. Nano Mater.* **2023**, *6*, 5136–5144.
10. Yu, X.; Mei, J.; Du, Y.; Cheng, X.; Wang, X.; Wu, Q. Engineered Interface of Three-Dimensional Coralliform NiS/FeS_2 Heterostructures for Robust Electrocatalytic Water Cleavage. *Nano Res.* **2023**, 5, 740-9.
11. Prakash, C.; Sahoo, P.; Yadav, R.; Pandey, A.; Singh, V.K.; Dixit, A. Nanoengineered Zn-Modified Nickel Sulfide (NiS) as a Bifunctional Electrocatalyst for Overall Water Splitting. *Int. J. Hydrogen Energy* **2023**, *48*, 21969–21980.

12. Wang, Q.; Du, X.; Zhang, X. Construction of CoS/NiS@CuS with Dandelion Flower-like Heterostructures as Efficient Catalysts for Overall Urea Splitting. *Int. J. Hydrogen Energy* **2023**, *48*, 24342–24355.
13. Tong, X.; Liao, W.; Zhai, Y.; Liu, P.; Yang, Q.; Chen, T. NiO/Co_2P Nanosheets with Heterogeneous Structure as a Multifunctional Catalyst for Overall Water Splitting . *J. Electrochem. Soc.* **2023**, *170*, 063509.